Available online at www.sciencedirect.com

ScienceDirect

Energy Procedia 40 (2013) 48 – 57

Energy Procedia

European Geosciences Union General Assembly 2013, EGU

Division Energy, Resources & the Environment, ERE

Spatio-temporal complementarity between solar and wind power in the Iberian Peninsula

S. Jerez[a]*, R. M. Trigo[a], A. Sarsa[b], R. Lorente-Plazas[c], D. Pozo-Vázquez[d], J. P. Montávez[c]

[a]*IDL, Faculdade de Ciências, Universidade de Lisboa, Campo Grande (Edificio C8), 1749-016 Lisboa, Portugal*
[b]*Departamento de Física, Universidad de Córdoba, Campus de Rabanales (Edificio C2), E-14071 Córdoba, Spain*
[c]*Departamento de Física, Universidad de Murcia, Campus de Espinardo (CIOyN), E-30100 Murcia, Spain*
[d]*Departamento de Física, Universidad de Jaén, Campus Lagunillas (Edificio A3), E-23071 Jaén, Spain*

Abstract

This study addresses the task of identifying optimum locations for solar and wind power plants so that the wind-plus-solar power generation meets certain conditions of efficiency and stability, thus allowing to overcome the downside that the natural variability of these renewable resources represents. The method was based on a simulated annealing algorithm and applied over the Iberian Peninsula, a region whose commitment to renewable energy is growing relatively fast. Obtained results are encouraging since a number of different sensitivity experiments support the spatio-temporal complementarity between solar and wind power, at least at the monthly time-scale, in this region.

Selection and peer-review under responsibility of the GFZ German Research Centre for Geosciences

Keywords: wind power; solar power; complementarity; optimization; Iberian Peninsula

1. Introduction

Investments on renewable energy installations are justified in both environmental and economic terms. On the one hand, climate change risks claim for mitigation strategies aimed at reducing CO_2 emissions [1]

* Corresponding author.
E-mail address: Sonia.jerez@gmail.com..

1876-6102
Selection and peer-review under responsibility of the GFZ German Research Centre for Geosciences
doi:10.1016/j.egypro.2013.08.007

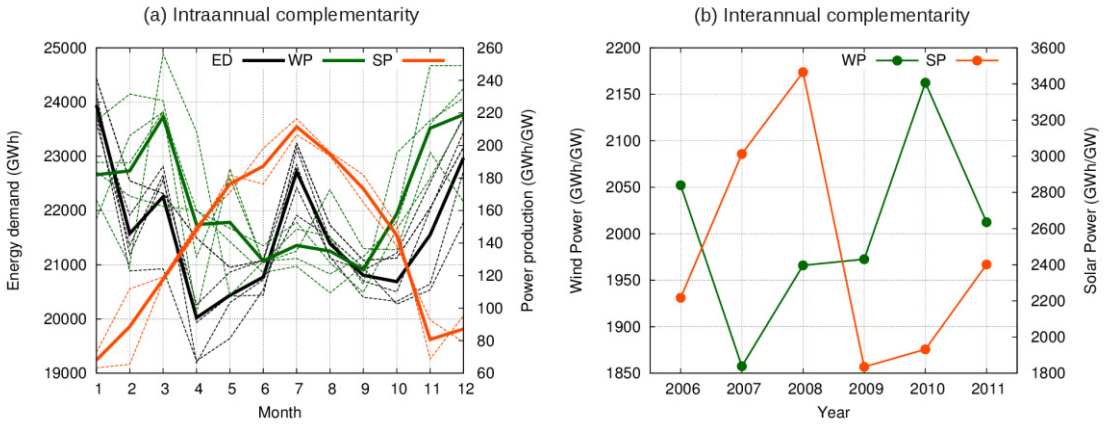

Fig. 1. (a) Annual cycles of energy demand (black, left y-axis) and wind (green) and solar (orange) power generation normalized by the installed power of each technology (right y-axis) in Spain. Solid lines depict mean values averaged for the last five years (two years, 2010 and 2011, in the case of solar power since monthly data of solar power are not available for longer) and dashed lines depict the annual cycles corresponding to these last five or two years in each case. (b) Annual values of wind (green, left y-axis) and solar (orange, right y-axis) power generation normalized by the installed power of each technology in each year in Spain. Data source: *www.ree.es*.

such as the so-called 20-20-20 target set by the European Union that commits to a 20% increase in renewable by 2020 compared with 1990 levels. On the other hand, renewable energies promote local employment and reduce the costly import of non-renewable energy resources [2,3]. Portugal and Spain are particularly sensitive to these concerns, having strongly funded wind farms during the last decades and more recently also solar plants [4,5].

Both wind and solar are weather and climate-dependent resources, thus presenting a natural temporal variability at time scales ranging from minutes-hours to seasons and years [6,7,8,9,10]. This fluctuating nature represents a major issue for the development of renewables since could lead to blackouts and thus implies the necessity of backup power systems. Besides, intermittent production creates negative externals that translate into grid integration costs [11,12]. The balancing and backup costs derived from this feature reduce the competitiveness of these energies as current power system operation is running a supply on demand system that is expected to be absolutely reliable. Hence, the challenge of identifying the ideal share of the different renewables guaranteeing a high efficiency (adjusted to the energy demand) without much temporal variations, as well as the best spatial location of the renewable energy plants for a particular country/region in that sense, needs to be addressed through comprehensive resource evaluation and holistic approaches [7,13,14,15,16,17].

The annual cycle of energy demand in Spain presents maxima in winter and summer, and neither the wind nor the solar power generation annual cycle alone adjusts to such annual profile (Fig 1a). Nevertheless, since the former is maximum in winter and the latter in summer, a combination of both could better match the energy demand curve. Moreover, we are relatively confident that this wind-plus-solar energy production could be reasonably constant in time, i.e. without too much variability from one year to another, given that the annual series of the energy production from both resources correlate negatively (Fig 1b).

Encouraged by this detected potential complementarity, the objective of this study is to develop and test a method to identify the optimal spatial distribution of wind and solar power plants across the Iberian Peninsula (IP) so that the combined wind-plus-solar yield meets the condition of minimum temporal

variability (in particular, at the monthly time-scale) under the constraint of a certain efficiency (i.e. achievement of a notably percentage of the energy demand).

Data employed are described in Section 2, the method in Section 3 and the results in Section 4. The main conclusions are drawn in Section 5.

2. Data

2.1. Raw wind and solar radiation data

The raw data consist of hourly series for the period 1959-2007 of incoming surface short-wave radiation (G) and wind speed (v), this later being available at several altitudes. These series are provided over a regular spatial grid covering the whole IP (including the Balearic Islands) with a horizontal resolution of 10 km. They were obtained from a hindcast regional climate simulation performed with the mesoscale model MM5 [18] driven by the ERA40 reanalysis [19] until 2002 (the last year that ERA40 spans) and by analysis data from the European Centre for Medium Range Weather Forecast (ECMWF) afterwards. Previous tests and works based on this simulation have shown its reliability for the purpose of this study [9,20].

2.2. Conversion of the raw data into wind and solar power

In order to convert the raw series of G and v into series of solar and wind power we have followed the set of rules proposed by [16] (Eqs. 1 and 2 respectively). The conversion is done at the original hourly resolution of the raw series. After, the resulting series were monthly averaged. This is particularly relevant in the case of the wind power since the relationship expressed in Eq. 2 is instantaneous and may not work at longer time-scales (e.g. monthly).

$$SP = \frac{G}{G_{STC}} \cdot P_R \tag{1}$$

$$\mathrm{WP} = \begin{cases} 0 & if \quad v < v_I \\ \dfrac{v^3 - v_I^3}{v_R^3 - v_I^3} & if \quad v_I \le v < v_R \\ 1 & if \quad v_R \le v < v_O \\ 0 & if \quad v \ge v_O \end{cases} \tag{2}$$

In Eq. 1 G_{STC} denotes the incoming surface short-wave radiation at standard conditions (G_{STC} = 1000 W/m^2) and P_R is the performance ratio accounting for system losses (typically 0.75). In Eq. 2 v_I denotes the cut-in speed (taken as 4 m/s), v_R the rated speed (12 m/s) and v_O the cut-off speed (25 m/s) of the turbine. These specifications correspond to one of the most common commercial turbines being used in Iberia, the model G87 from the Gamesa Corporation (*www.gamesa.es*), whose power rated is 2 MW and both the rotor diameter and the tower height are 87 m. Hence, the wind speed data were retrieved from the fourth vertical sigma level of the simulated database (sigma is the vertical variable employed in MM5)

whose altitude across the domain is around 100 meters, the closest to the turbine height.

Eqs. 1 and 2 provide normalized values, i.e. power generation per unit of power installed, thus ranging from 0 to 1. In order to quantify the power generated per grid cell, we will consider that each grid cell can have either solar or wind plants occupying 1/4 of its area (which is 100 km^2). Based on the specifications of [16], this consideration results on solar (wind) plants with 1250 (135) MW of installed capacity in each grid cell.

3. Methodology

The monthly series of solar and wind power from each grid cell are the inputs for the optimization algorithm applied in this work. In addition, the following parameters should be specified:

- Maximum number of grid cells to be chosen for having solar (wind) plants, NS_{max} (NW_{max})
- Minimum number of grid cells to be chosen for having solar (wind) plants, NS_{min} (NW_{min})
- Total number of grid cells to be chosen for having either solar or wind plants, $N \leq NS_{max} + NW_{max}$
- Minimum mean power production required from the set of N installations, $\overline{P}_{min}$

Then the algorithm, based on simulated annealing [21], identifies NS grid cells for having solar plants and NW grid cells for having wind plants (overlapping is allowed, i.e. we can have both solar and wind plants in the same cell), with $NS_{min} \leq NS \leq NS_{max}$, $NW_{min} \leq NW \leq NW_{max}$ and $NS+NW=N$, so that the sum of the total solar power production in the NS cells, SP, plus the total wind power production in the NW cells, WP, denoted as P ($P=SP+WP$), verifies that:

(1) $\overline{P} \geq \overline{P}_{min}$

(2) $\sigma(P)$ is minimum among all the possible combinations of grid cells that could have been chosen for having solar and/or wind plants.

with $\overline{P}$ and $\sigma(P)$ being the mean and the standard deviation of the P series.

We have used the optimization algorithm in three different modes:

a) S mode: the former conditions (1) and (2) are verified considering only solar plants (this is achieved by imposing $NW_{max}=0$),
b) W mode: analogous to the S mode but considering only wind plants ($NS_{max}=0$),
c) SW mode: the algorithm is totally free when looking for the optimum choice of grid cells and the optimum combination of both powers ($NS_{max}=NW_{max}=N$).

This provides a framework to compare the results obtained in each mode.

Moreover, from a methodological perspective we have adopted two fairly different approaches when applying the algorithm. First we have considered all the grid cells over the IP and the Balearic Islands (5538) and looked for the optimum solar and wind power locations for each month separately (Section 4.1). Hence, we used the optimization algorithm to minimize the interannual variability of the monthly power production series. Although the locations selected by the algorithm for solar and wind power plants will differ from one month to another, which is not particularly useful, this approach highlights the maximum potential of the method. Second, we have attempted a more realistic approach by (1) preselecting those grid cells whose mean values of the solar and wind power series stands above the median (a total of 2769 grid cells in each case), and (2) considering the entire year of solar and wind power monthly series without splitting these by months (Section 4.2). This second approach will provide a unique distribution for the solar and wind installations across the IP, while the interannual variability of the monthly power production series will not be as low as in the first approach.

Finally, we have considered different stages of renewable energy penetration by taking N varying in 200, 400, 600, 800 and 1000 installations, and monthly values for $\overline{P}_{min}$ varying in 20%, 40%, 60%, 80% and 100% of the mean energy demand of each month (black line in Fig 1a).

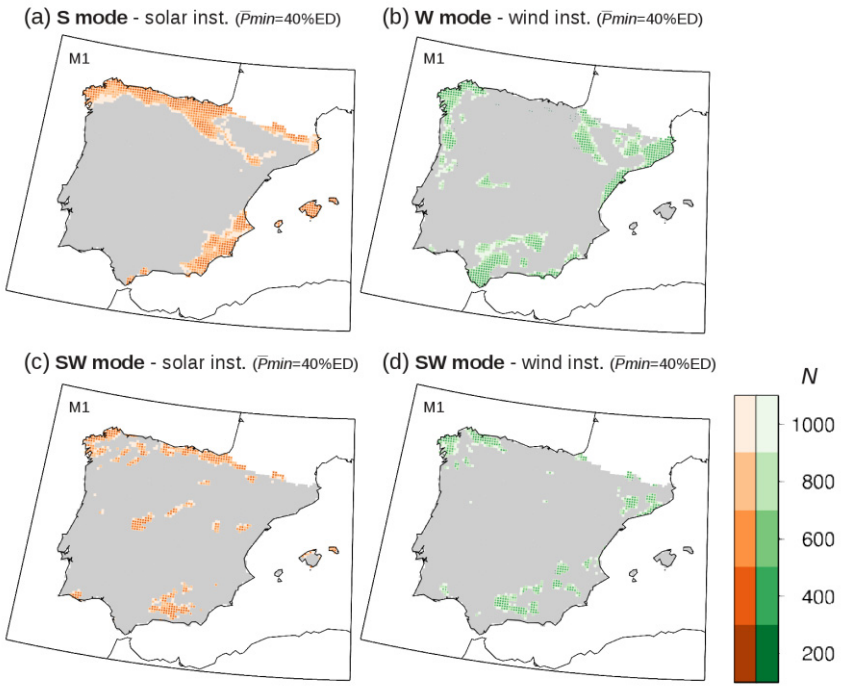

Fig. 2. Grid cells selected by the optimization algorithm for the installation of solar (orange) and wind (green) power plants in order to minimize the variability of the monthly production series of January ensuring a minimum mean production ($\overline{P}_{min}$) of at least 40% of the mean energy demand (ED) in January. The algorithm was applied in (a) the S mode, (b) the W mode and (c,d) the SW mode. *N* varies in 200, 400, 600, 800 and 1000 number of installations (see color palette). The non-selected locations remain shaded in gray. White areas were not considered.

4. Results

4.1. Idealistic approach

First, the algorithm was applied for the monthly series of solar and wind power of each month separately and considering all the grid cells in the IP. As an example, Fig 2 shows the distribution of solar and wind power plants that minimizes the interannual variability of the monthly production series of January ensuring a mean power production of at least 40% of the mean energy demand in this month. Beyond the spatial distribution achieved (that will vary when considering a different month), it is worth noting its stability in the three modes despite the different values of *N*, and also despite the value of $\overline{P}_{min}$ (not shown). This tendency to congregate the winning sectors in clusters stands also for the rest of months.

Mantaining the former example, Fig 3 shows explicitly the gain achieved in terms of reduction of $\sigma(P)$ from the wind-plus-solar approach in comparison to either the only-wind or the only-solar approaches. Since the *SP* and *WP* series obtained in the SW mode (dashed lines) are strongly anticorrelated, the *P* series in the SW mode (blue solid line) depict a much more constant temporal evolution than the *P* series obtained in both the S and the W modes (orange and green solid lines, respectively). Interestingly, the *SP* series from the S mode and the *WP* series from the W mode are also clearly anticorrelated, which supports the overwhelmed interannual complementarity between both resources across the IP, as it was also appreciable in Fig 1b. Indeed, this complementarity has been largely attributed to the opposite

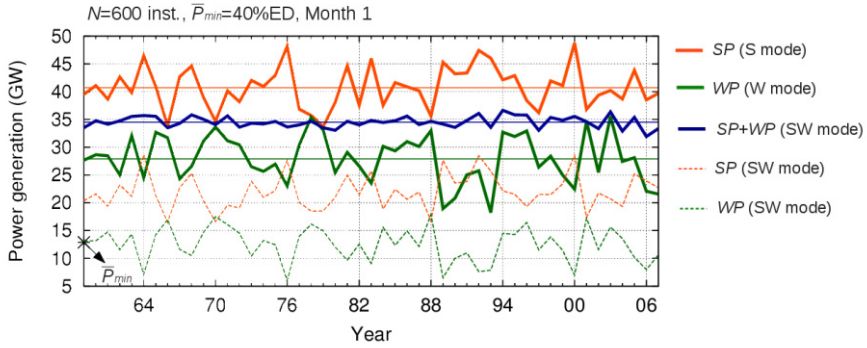

Fig. 3.Power generation series in January obtained from the locations shown in Fig 2 for N=600 installations. The orange lines depict solar power generation in the S mode (solid line) or the SW mode (dashed line). The green lines depict wind power generation in the W mode (solid line) or the SW mode (dashed line). The blue line depicts solar-plus-wind power generation in the SW mode (it is the sum of the dashed orange and green lines).

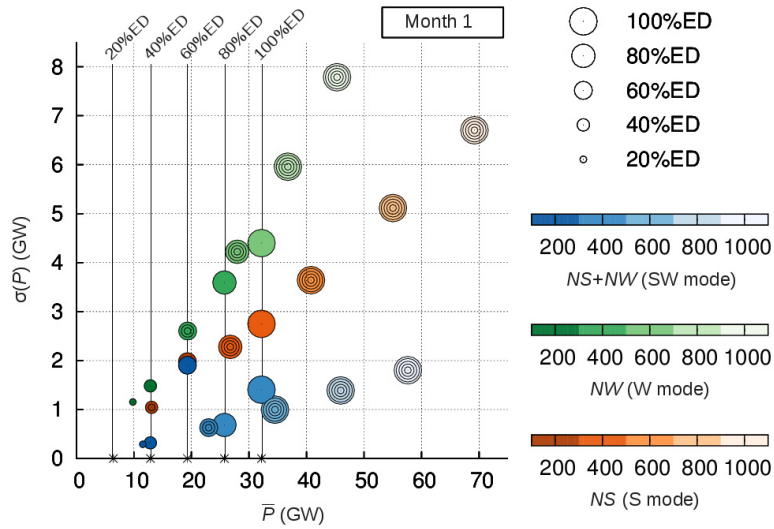

Fig. 4. σ(P) versus $\overline{P}$ as they are obtained from various executions of the optimization algorithm in the S mode (orange), the W mode (green) and the SW mode (blue) for N varying in 200, 400, 600, 800 and 1000 installations (indicated by the color intensity) and $\overline{P}_{min}$ varying in 20%, 40%, 60%, 80% and 100% of the mean energy demand (ED) in January (indicated by the bubbles size), with the inputs being the monthly solar and wind power series of January of all the grid cells over the IP.

response of both resources to main large-scale circulation modes driven the Iberian climate such as the North Atlantic Oscillation, the East Atlantic and the Scandinavian patterns [9,10]. It should be also noted the different value of $\overline{P}$ obtained in each mode (beelines in Fig 3). This will be recalled later.

By plotting σ(P) versus $\overline{P}$ for all the N- $\overline{P}_{min}$ pairs considered (Fig 4), we ascertain the advantage of the SW mode in comparison to both the S and the W modes for all the tested cases. As expected, higher values of $\overline{P}$ implies higher values of σ(P), being this relationship quite linear in Fig 4 and showing the smallest slope for the SW mode (i.e. for the same increment in $\overline{P}$, σ(P) increases less in the SW mode than in the S mode, and less in this latter than in the W mode). Note that for some cases the solutions overlap. This occurs when the minimum σ(P) has already associated a high value of $\overline{P}$.

For the sake of brevity, the results shown in Figs 2 to 4 for January are not provided for the rest of

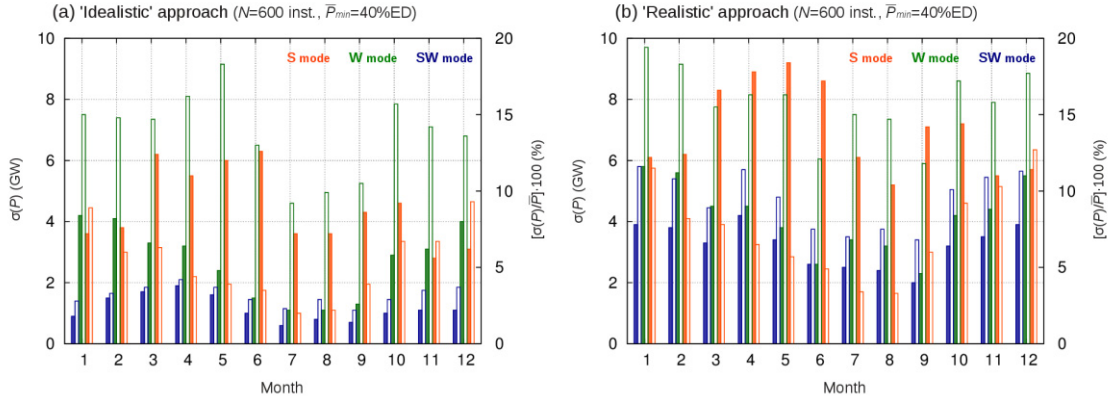

Fig. 5. Standard deviation of the total production (P) series that result from (a) the idealistic and (b) the realistic execution of the optimization algorithm in the S mode (orange), the W mode (green) and the SW mode (blue) for N=600 installations and $\overline{P}_{min}$=40% of the mean energy demand in each month. Solid boxes depict σ(P) being referred to the left y-axis. Empty boxes depict (σ(P)/$\overline{P}$)·100 being referred to the right y-axis.

months, although the same analysis has been done for all of them. However, in order to show that the variance of P is valuably reduced in the SW mode compared to the single-power approaches in all months, Fig 5a depicts the values of σ(P) (left y-axis) and σ(P) normalized by $\overline{P}$ (right y-axis) obtained in the three modes for each month. In absolute (relative) terms, the variance of the P series shows maxima in winter in the W (S) mode. In the rest of the cases, the variance is generally larger in the transitional seasons (spring and autumn). In all months, in both absolute and relative terms, the variance of the P series obtained in the SW mode is the smallest, with the only exceptions of the normalized σ(P) in July and August, which is smallest in the S mode. Besides, small variations throughout the year of both σ(P) and normalized σ(P) can be observed in the SW mode, in contrast with the pronounced seasonal variations obtained in the S and W modes. As a reference, the variance of the production series from the optimum combination of solar and wind power plants identified by the algorithm in this experiment remains below the 5% of the mean production in all months.

4.2. Realistic approach

In this Section we identify single sets of locations that minimize the variability of the complete series (i.e. without splitting them by months). For these runs of the algorithm we have discarded those locations having mean solar or wind power production values below the 50th percentile computed for the whole IP and the Balearic Islands, thus adopting a more realistic and conservative approach as planers and private investors will tend to dismiss less productive regions. As Fig 2, Fig 6 shows the selected locations for the various values of N and for $\overline{P}_{min}$ equals to the 40% of the mean energy demand in each month (in gray are the areas that, although passing the filter of the 50th percentile in mean production, were not selected). The S mode places the solar power plants along the south and east Iberian coastlines. The W mode selects the Ebro river valley (in the north-east of the IP), coastal areas in the south-west and some mountain ranges in the north-west. In the SW mode, the greatest load falls on the wind power, with the spatial distribution of wind plants being very similar to that obtained in the W mode, while few locations are selected for having solar power installations. This indicates the good complementarity among different regions within the IP of the wind power alone. However, it should be noted that in the most demanding cases (i.e. small N and high $\overline{P}_{min}$) the W mode does not provide solutions. As it was also outstanding in the results from the idealistic runs of the previous Section, the spatial patterns in Fig 6 are relatively invariant under changes in the specifications of N and $\overline{P}_{min}$.

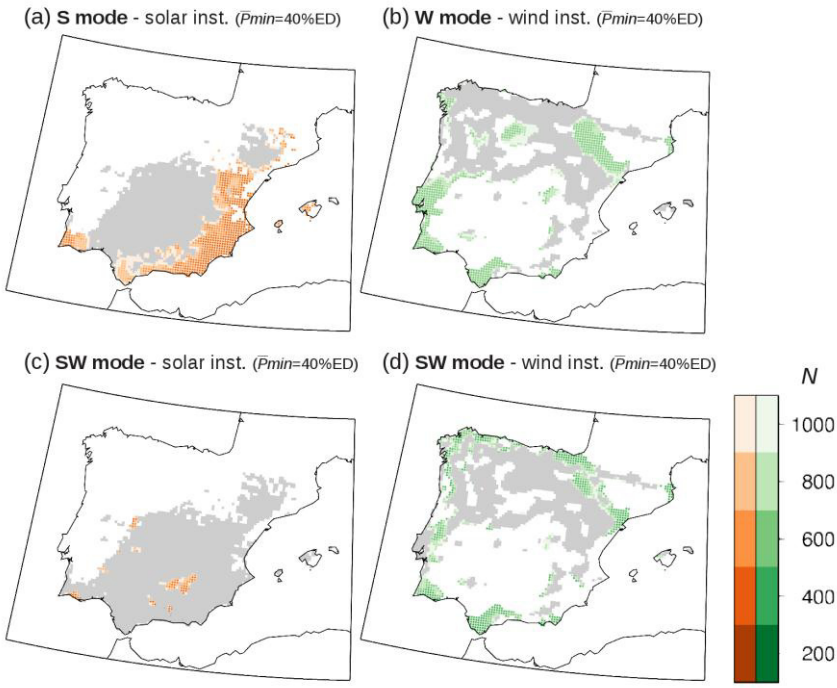

Fig. 6. Grid cells selected by the optimization algorithm for the installation of solar (orange) and wind (green) power plants in order to minimize the variability of the monthly production series (including all months from January to December) ensuring a minimum mean production ($\overline{P}_{min}$) of at least 40% of the mean energy demand (ED) in each month. The algorithm was applied in (a) the S mode, (b) the W mode and (c,d) the SW mode. *N* varies in 200, 400, 600, 800 and 1000 number of installations (see color palette). The non-selected locations remain shaded in gray. White areas were not considered.

Finally, we have evaluated the interannual variability of the resulting monthly *P* series (Fig 5b). Qualitatively, the results are very similar to those obtained with the idealistic runs (Fig 5a), with the variance of the monthly *P* series being overall higher in the winter half of the year. The wind-plus-solar combination reduces not only the variance of the series for all months (that, in the shown case, ranges between 5 and 10% of $\overline{P}$) but also such seasonality. Note that the S mode shows the worst performance as it provides the highest values of $\sigma(P)$, although this changes radically when the variance is expressed in relative terms since it provides also the highest values of $\overline{P}$ (recall the last comment on Fig 3). From this perspective it would seem that the S mode surpasses the SW mode, but this is just because the SW mode adjusts better to $\overline{P}_{min}$ and because what we have implemented in the algorithm is the condition of minimum $\sigma(P)$, not of minimum $\sigma(P)/\overline{P}$. Actually, the SW mode would provide the same solution than either the S or the W mode in case it was the best attending to the condition imposed.

5. Conclusions

The Iberian Peninsula shows a strong potential in terms of complementarity between solar and wind power. Here we faced the challenge of identifying optimum spatial distributions for solar and wind plants in order to guarantee a certain energy generation but ensuring the minimum inter-annual and seasonal temporal variations. For this purpose we have customized a simulated annealing algorithm and applied it using solar and wind power series provided in a homogeneous grid covering the whole Iberian Peninsula with 10 km resolution.

Several experiments, considering different stages of penetration of the renewable energies and different efficiency conditions, were performed. The results demonstrate the capability of the method, being able to profitably reduce the interannual variability of the monthly power generation series that result from an optimum wind-plus-solar power system, also enhancing its stability throughout the year, in comparison to the single-source approaches.

The algorithm has been implemented so that it is highly flexible and accepts the inclusion of different types of restrictions, conditions or assumptions, e.g. changes in the predefined values of $\overline{P}_{min}$, to take into account already existing installations, the exclusion of particular areas such as national parks, etc. In particular, in the case of Iberian Peninsula, to take into consideration the large amount of existing wind power farms [8,9] in future assessments would be very interesting from a practical point of view.

Moreover, although the method has been applied here for the Iberian Peninsula using monthly values of power generation, the algorithm is perfectly adaptable to other time-scales and other regions. By demonstrating the plausibility of the proposal and given their economical and environmental relevance, our results encourage further research focused on, for instance, finer time-scales (e.g. daily) and/or wider regions (e.g. Europe or USA).

Acknowledgements

This study was supported by the Portuguese Science Foundation (FCT) through the project 'ENAC' (PTDC/AAC-CLI/103567/2008) and by the Spanish MEC and FEDER through the projects 'Minieólica' (PSE.120000.2007.14) and FIS2012-39617-C02-02.

References

[1] IPCC WG III. Climate change 2007: mitigation of climate change. In: Metz B, Davidson OR, Bosch PR, Dave R, Meyer LA, editors. *Contribution of Working Group III to the Fourth Assessment Report of the Intergovernmental Panel on Climate Change*, Cambridge and New York: Cambridge University Press; 2007.

[2] Moreno B, López AJ. The effect of renewable energy on employment. The case of Asturias (Spain). *Renew Sust Energ Rev 2008*;**12**(3):732–751.

[3] Bhattacharyya SC. Fossil-fuel dependence and vulnerability of electricity generation: Case of selected European countries. *Energy Policy 2009*;**37**(6):2411–2420.

[4] Ridao AR, García EH, Escobar BM, Toro MZ. Solar energy in Andalusia (Spain): present state and prospects for the future. *Renew Sust Energ Rev 2007*;**11**(1):148–161.

[5] Río González P. Ten years of renewable electricity policies in Spain: An analysis of successive feed-in tariff reforms. *Energy Policy 2008*;**36**(8):2917–2929.

[6] Pozo-Vázquez D, Tovar-Pescador J, Gámiz-Fortis SR, Esteban-Parra MJ, Castro-Díez Y. NAO and solar radiation variability in the European North Atlantic region. *Geophys Res Lett 2004*;**31**(5):L05201.

[7] Brayshaw DJ, Troccoli A, Fordham R, Methven J. The impact of large scale atmospheric circulation patterns on wind power generation and its potential predictability: A case study over the UK. *Renew Energ 2011*;**36**(8):2087–2096.

[8] García-Bustamante E, González-Rouco JF, Navarro J, Xoplaki E, Luterbacher J, Jiménez PA, Montávez JP, Hidalgo A, Lucio-Eceiza EE. Relationship between wind power production and North Atlantic atmospheric circulation over the northeastern Iberian Peninsula. *Clim Dyn 2013*;**40**(3-4):935–949.

[9] Jerez S, Trigo RM, Vicente-Serrano SM, Pozo-Vázquez D, Lorente-Plazas R, Lorenzo-Lacruz J, Santos-Alamillos F, Montávez JP. The impact of the North Atlantic Oscillation on the renewable energy resources in south-western Europe. *J Appl Meteorol Climatol 2013;* submitted.

[10] Jerez S, Trigo RM. Time-scale and extent at which large-scale circulation modes determine the wind and solar potential in

the Iberian Peninsula. *Environ Res Lett 2013;* submitted.

[11] Lund H. Large-scale integration of wind power into different energy systems. *Energy 2005*;**30**:2402–2414.

[12] Lund H. Large-scale integration of optimal combinations of PV, wind and wave power into the electricity supply. *Renew Energ 2006*;**31**:503–515.

[13] Archer CL, Jacobson MZ. Supplying Baseload Power and Reducing Transmission Requirements by Interconnecting Wind Farms. *J Appl Meteorol Climatol 2007*;**46**:1701–1717.

[14] Heide D, Von Bremen L, Greiner M, Hoffmann C, Speckmann M, Bofinger S. Seasonal optimal mix of wind and solar power in a future, highly renewable Europe. *Renew Energ 2010*;**35**(11):2483–2489.

[15] Delucchi MA, Jacobson MZ. Providing all global energy with wind, water, and solar power, Part II: Reliability, system and transmission costs, and policies. *Energy Policy 2011*;**39**(3):1170–1190.

[16] Ruiz-Arias JA, Terrados J, Pérez-Higueras P, Pozo-Vázquez D, Almonacid G. Assessment of the renewable energies potential for intensive electricity production in the province of Jaén, southern Spain. *Renew Sust Ener Rev 2012*;**16**(5):2994–3001.

[17] Santos-Alamillos FJ, Pozo-Vázquez D, Ruiz-Arias JA, Lara-Fanego V, Tovar-Pescador J. Analysis of spatiotemporal balancing between wind and solar energy resources in the southern Iberian Peninsula. *J Appl Meteorol Climatol 2012*;**51**:2005–2024.

[18] Grell GA, Dudhia J, Stauffer DR. *A description of the fifth-generation Penn State/NCAR Mesoscale Model (MM5).* NCAR Tech. Note 398+STR, Natl. Cent. For Atmos. Res., Boulder, Colo; 1994.

[19] Uppala SM, Källberg PW, Simmons AJ, Andrae U, Bechtold V, Fiorino M, Gibson JK, Haseler J, Hernandez A, Kelly GA, Li X, Onogi K, Saarinen S, Sokka N, Allan RP, Andersson E, Arpe K, Balmaseda MA, Beljaars ACM, Van De Berg L, Bidlot J, Bormann N, Caires S, Chevallier F, Dethof A, Dragosavac M, Fisher M, Fuentes M, Hagemann S, Hólm E, Hoskins BJ, Isaksen L, Janssen PAEM, Jenne R, Mcnally AP, Mahfouf JF, Morcrette JJ, Rayner NA, Saunders RW, Simon P, Sterl A, Trenberth KE, Untch A, Vasiljevic D, Viterbo P, Woollen J. The ERA-40 re-analysis. *Q J Roy Meteor Soc 2005*;**131**:2961–3012.

[20] Lorente-Plazas R, Montávez JP, Jerez S, Gómez-Navarro JJ, Jiménez-Guerrero P, Jiménez PA, García-Valero JA, Gomáriz-Castillo F, Alonso-Sarría F. EOLMAP: A web tool to assess the wind resource over Spain. In: Fernández F, Galián E, Cañada R, editors. *Interantional conference on renewable energies and power quality (ICREPQ' 12),* Santiago de Compostela, Spain: Publicaciones de la AEC - Serie A; 2012, 7(I):95-105.

[21] Press WH, Teukolsky SA, Vetterling WT, Flannery BP. *Numerical Recipes in FORTRAN: The art of scientific computing*. Cambridge University Press; 1992.